Journal of Nuclear Materials 390–391 (2009) 404–407

Contents lists available at ScienceDirect

Journal of Nuclear Materials

journal homepage: www.elsevier.com/locate/jnucmat

Self-consistent modeling of impurity seeded JET advanced tokamak scenarios

R. Zagórski [a,*], G. Telesca [b], G. Arnoux [c], M. Beurskens [c], W. Fundamenski [c], K. McCormick [d], JET-EFDA Contributors [1]

[a] Institute of Plasma Physics and Laser Microfusion, EURATOM Association, Warsaw, Poland
[b] Institute for Energy Research – Plasma Physics, Forschungszentrum Jülich, Germany
[c] EURATOM/UKAEA Fusion Association, Culham Science Center, Abingdon, UK
[d] Max-Planck Institute of Plasma Physics, Garching, Germany

ARTICLE INFO

PACS:
52.25.Fi
52.25.Vy
52.40.Hf
52.55.Fa
52.65.Kj

ABSTRACT

The influence of neon and nitrogen seeding on the divertor heat load in JET tokamak is studied in terms of the numerical simulations of the whole device by the self-consistent core–edge code COREDIV and results are presented for advanced tokamak scenarios. First, the code has been applied to simulate two JET shots (#69980, #69987) characterized by different radiation levels. With this basis the code is used next to provide guidance for the JET experiments in terms of: effects on the heat load at the target plates for various x-point positions with respect to the target plates, and the effect of higher plasma and separatrix density, as well as effects of pure or mixed Ne/N_2-seeding.

1. Introduction and transport model

The reduction of divertor target power loads to an acceptable level is an important issue for the new ITER Like Wall (ILW) JET configuration, in particular for advanced tokamak (AT) scenarios. Such discharges are characterized usually by relatively low densities and high powers and as a consequence, low recycling, hot plasma conditions are established in the edge region where even partial divertor detachment is difficult to achieve both inboard and outboard. This might lead to serious consequences for the plasma facing components of the future all-metal ILW planned at JET since the use of W as divertor target material will remove carbon as a strong natural radiator. Therefore, to reduce the heat load on the divertor, impurity injection (Ne/N_2) techniques have to be developed and investigated.

This paper describes integrated numerical modelling applied for the first time to JET AT discharges using the COREDIV code [1] being able to describe self-consistently the core and edge plasmas. The code results have been compared with the nitrogen seeded type III ELMy H-mode JET discharges [2,3], which have a similar geometry but different parameter space than AT scenarios. Here, we concentrate on numerical simulations of Ne and N seeded JET AT scenarios, which in contrast to type III ELMy discharges, are characterized by lower plasma densities and smaller radiation fractions. The COREDIV code is used to provide guidance for the JET experiments in terms of: effects on the heat load at the target plates for various x-point positions with respect to the target plates, the effect of plasma and separatrix densities, and effects of Ne/N_2-seeding.

The physical model used in the COREDIV code is based on a self-consistent coupling of the radial transport in the core to the 2D multifluid description of the scrape-off layer. Since the model is relatively complex, and has been already presented elsewhere [1] we point out here only on the most important aspects of the model.

In the core, the 1D radial transport equations for bulk ions, for each ionization state of impurity ions and for the electron and common ion temperature are solved. For auxiliary heating a parabolic-like deposition profile is assumed whereas the energy losses are determined by bremsstrahlung and line radiation. The equation for the poloidal magnetic field has been neglected and thus the current distribution is assumed to be given in our approach. The electron and ion energy fluxes are defined by the local transport model proposed in Ref. [4] which reproduces a prescribed energy confinement law. In particular, the anomalous heat conductivity is given by the expression $\chi_{e,i} = C_{e,i}\frac{a^2}{\tau_E}\left[1+\left(\frac{r}{a}\right)^4\right]$ where τ_E is the energy confinement time defined by the ELMy H-mode scaling law [5], a is the plasma radius and $C_e = C_i = 0.27$ in the present simulations in order to have agreement between calculated and experimental confinement times. The profile of the main plasma ion density is given by the solution of the radial diffusion equation with diffusion coefficients $D_e = D_i = 0.5\chi_e$ chosen to reproduce the shot 69 987. The source term takes into account the attenuation of the neutral density due to ionization processes: $S_i = S_{i0}\exp(-\frac{a-r}{\lambda_{ion}})$,

* Corresponding author. Address: EFDA CSU – Garching, Max-Planck-Institut für Plasmaphysik, Boltzmannstr. 2, D-85748 Garching Bei München, Germany.
E-mail address: Roman.Zagorski@efda.org (R. Zagórski).

[1] See the Appendix of M.L.Watkins et al., Fusion Energy 2006 (Proc. 21st Int. Conf. Chengdu, 2006) IAEA, (2006).

0022-3115/$ - see front matter © 2009 Elsevier B.V. All rights reserved.
doi:10.1016/j.jnucmat.2009.01.099

where λ_{ion} is the penetration length of the neutrals, calculated self-consistently. The source intensity S_{i0} is determined by the internal iteration procedure in such a way that the volume average electron density defined by neutrality condition equals to that from experiment. The radial impurity transport is described by standard neoclassical (collisionality dependent) and anomalous transport.

In the SOL we use the 2D boundary layer code EPIT which is primarily based on Braginskii-like equations [6]. In the past, the EPIT code was used to analyze plasma parameters in the limiter configuration of FTU tokamak resulting in satisfactory agreement between calculated and measured quantities [7]. For every ion species the continuity, the parallel momentum and energy equations are solved and an analytical description of the neutrals allows the inclusion of plasma recycling as well as the sputtering processes at the target plates. We assume that the divertor is in attached (semi-attached) mode and recycling coefficients of hydrogen and impurities are external parameters. Although the temperature is high at the strike points and, by consequence, physical sputtering is the dominant mechanism for impurity release, also the contribution of chemical sputtering of carbon is considered according to the Roth formula [8] giving in most cases the yield of the order of $Y_{chem} \sim 0.006$. A simple slab geometry (along magnetic field lines and radial direction) with classical parallel transport and anomalous radial transport ($D_i = \chi_i = 0.5\chi_e = 0.25\ m^2\ s^{-1}$) is used and the impurity fluxes and radiation losses caused by intrinsic and seeded impurity ions are calculated fully self-consistently. We solved the equations only from the midplane to the plate assuming inner–outer symmetry of the problem.

The standard sheath boundary conditions are imposed at the plates, whereas at the wall the boundary conditions are given by decay lengths ($\lambda_n = 3$ cm, $\lambda_T = 4$ cm). The parallel velocities and the gradients of densities and temperatures are assumed to be zero at the midplane (stagnation point). The coupling between the core and the SOL is made by imposing continuity of energy and particle fluxes as well as of particle densities and temperatures at the separatrix.

2. Results of calculations and discussion

In the present paper, the COREDIV code is applied to investigations of advanced tokamak (AT) scenarios characterized by improved energy confinement due to the development of the internal transport barrier. Such operating regimes, however, are usually achieved at low plasma densities and thus impurity seeding is required to reduce the heat flow to the divertor plates. Neon and nitrogen seeding has been considered in the calculations.

First, in order to fix some of the code input parameters we have simulated two JET AT discharges with plasma current I_p = 1.9 MA, magnetic field B_T = 3.1 T, different volume average densities n_e and additional heating powers, P_{aux}. In Table 1, some global parameters of two discharges #69980 and #69987 are compared to simulation results and the agreement is satisfactory (note that experimental estimation of Z_{eff} is very crude). We note that in the shot #69887 with only intrinsic carbon impurity, the 'natural' carbon radiation is relatively low and the total radiation amounts only to 27% of the input power whereas in the shot #69980 injection of neon increases the radiation up to 40% of P_{aux}.

Table 1
Comparison of COREDIV results with experimental data. Here n_{e0}, T_{e0}, T_{i0} are plasma density, electron and ion temperatures in the center, respectively. Z_{eff} is the volume average effective charge and $f_{rad} \equiv P_{rad}/P_{tot}$ is the radiation fraction, where P_{rad} is the total radiation and P_{tot} is the total input power.

	#69980	COREDIV	#69987	COREDIV
$n_e \times 10^{19}$ m^{-3}	4.6	4.6	4.2	4.2
P_{aux} MW	24	24	21.8	21.8
$n_{e0} \times 10^{19}$ m^{-3}	5.7	5.3	4.9	4.9
Z_{eff}	3.4–6	3.4	2.1–4.6	3.15
f_{rad}	0.4	0.42	0.27	0.26
T_{e0} (keV)	5.2	4.7	5	5.2
T_{i0} (keV)	5.4	5.2	6	6
τ_E (s)	0.18	0.18	0.2	0.21

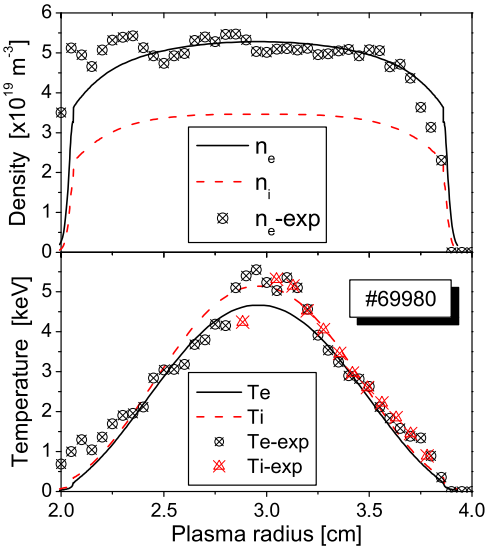

Fig. 1. Comparison of experimental and numerical profiles of the plasma densities and temperatures (electron and ion, respectively) for the JET shot #69980 ($P_{aux} = 24$ MW, $n_e = 4.6 \times 10^{19}$ m^{-3}).

In Figs.1 and 2 the calculated and experimental profiles of plasma density and temperature for the same shots are presented. It can be seen that plasma profiles are nicely reproduced by the code. We recall here that we have used a relatively simple transport model with prescribed profiles of transport coefficients (without pedestal), with free parameters fixed to reproduce JET pulse (#69987), but it comes from the calculations that the profile of the transport coefficients is not of primary importance as long as the transport is scaled in a way to reproduce the experimental energy confinement time.

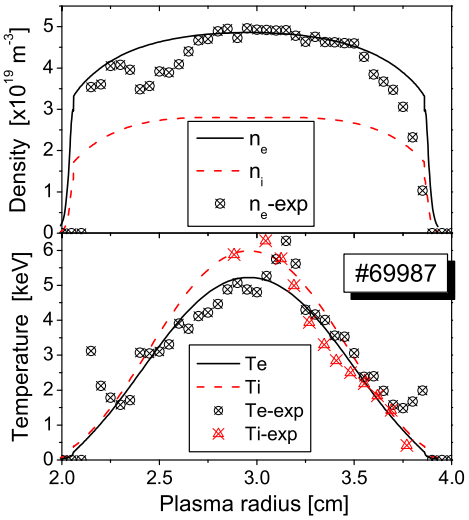

Fig. 2. Comparison of experimental and numerical profiles of the plasma densities and temperatures (electron and ion, respectively) for the JET shot #69987 ($P_{aux} = 21.8$ MW, $n_e = 4.2 \times 10^{19}$ m^{-3}).

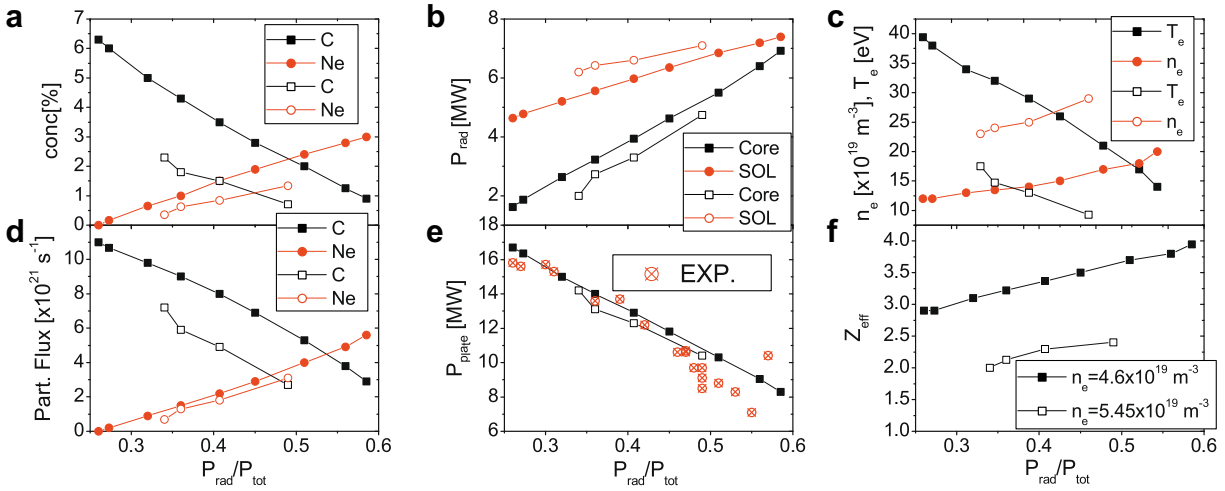

Fig. 3. Plasma parameters versus radiation fractions (Neon seeding): full symbols – $n_e = 4.6 \times 10^{19}$ m^{-3}, open symbols – $n_e = 5.45 \times 10^{19}$ m^{-3}; (a) volume averaged impurity concentration, (b) radiated power in the core and SOL regions, (c) plasma temperature and density at the plate (strike point), (d) impurity particle fluxes to the targets, (e) power to the divertor plates; calculated and measured and (f) volume averaged Z_{eff}.

Since it appears that the COREDIV code is able to reproduce core features of the AT plasma scenarios in JET, we have used the code to make parametric studies of JET discharges. Our interest has been focused on Neon and Nitrogen seeded discharges with carbon as the plate material. In Fig. 3 we show results of simulations corresponding to the AT JET scenarious with neon seeding for two different plasma densities: low density $n_e = 4.6 \times 10^{19}$ m^{-3} corresponds to already performed experiments whereas the higher density $n_e = 5.45 \times 10^{19}$ m^{-3} makes predictions for future discharges. In simulations we have changed the level of neon puffing (10^{20} s$^{-1} \leqslant \Gamma^{Ne}_{puff} \leqslant 9 \times 10^{20}$ s^{-1}) keeping all other parameters constant. However, the results are presented in the function of radiation fraction, f_{rad} ($\equiv P_{rad}/P_{tot}$) since that parameter can be easily measured in the experiment and in the considered range of gas puff levels it is almost linear function of the neon puffed flux.

The increase of neon level leads directly to the increase of the total radiated power and consequently corresponding reduction of the heat load to the target plates as seen also in the experiment (Fig. 3(e)). In Fig. 3(a) carbon and neon concentrations are shown, the plot nicely illustrates the interchange mechanism of replacing one impurity by another, also observed in the experiment [3]. It can be seen that the carbon concentration is reduced when the intensity of the neon source increases leading consequently to a relatively moderate increase of the Z_{eff} level. In fact the increased neon radiation cools the plasma edge and reduces carbon erosion (mostly the physical sputtering). It can be seen that for high radiation fractions the discharge is dominated by neon, whereas for lower radiation level carbon ions starts to be important. At low puffing levels the radiation comes mostly from the SOL (carbon does not radiate in the core plasma) but for neon dominated discharges a significant part of the plasma energy is radiated in the core.

It is interesting to note, that opposite to the expectations, the total radiated power does not depend on the plasma density (Fig. 3(b)), at least in the range of parameters considered in the paper. In fact, the SOL radiation increases when the plasma density increases but the core radiation is reduced and consequently the sum remains constant. The reduction of the core radiation can be associated to the improved screening efficiency of the SOL when density is increased. It is confirmed also by the smaller value of

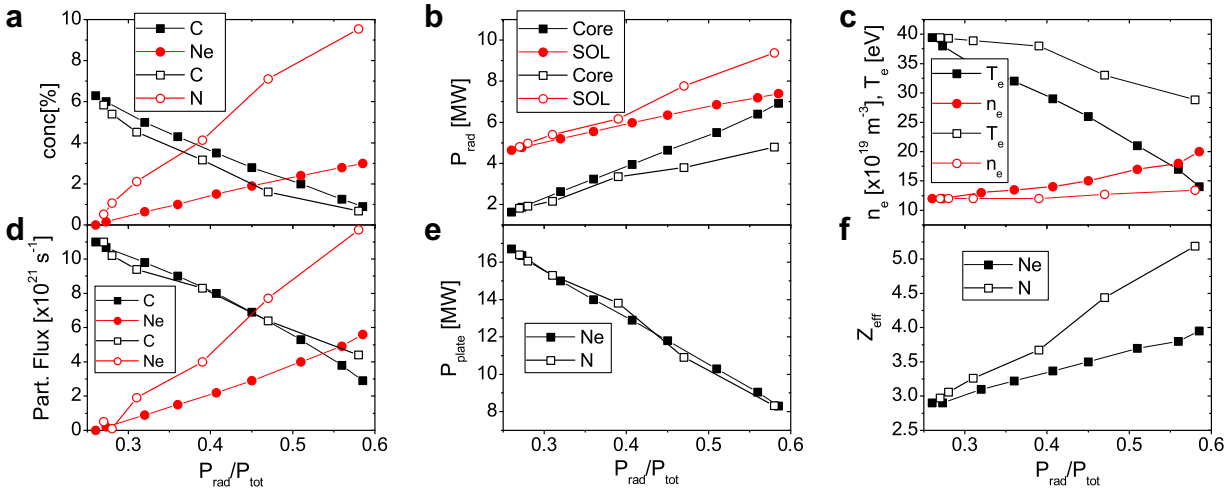

Fig. 4. Plasma parameters versus radiations fractions ($n_e = 4.6 \times 10^{19}$ m^{-3}): full symbols – Neon seeding, open symbols – Nitrogen seeding; (a) volume averaged impurity concentration, (b) radiated power in the core and SOL regions, (c) plasma temperature and density at the plate (strike point), (d) impurity particle fluxes to the targets, (e) power to the divertor plates and (f) volume averaged Z_{eff}.

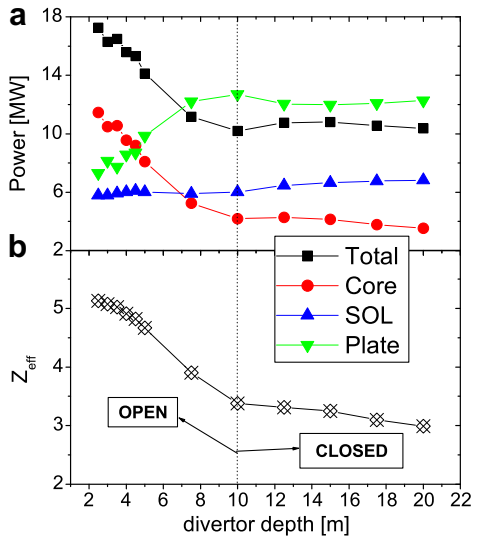

Fig. 5. Plasma parameters versus divertor depth (x-point to target distance along magnetic field line: (a) different powers: total radiation, radiation in the core and SOL regions, power to plate and (b) volume averaged Z_{eff}.

Z_{eff} as well as smaller concentration of impurities in the core. In Fig. 4 we show similar profiles but this time obtained with nitrogen seeding. Since the nitrogen is not a recycling impurity the core contamination depends on the source position and therefore we assumed the puff source in the divertor region in order to reduce the core contamination (for neon, as a recycling impurity the position of the source does not influence core parameters as was already shown in [2]). It is important to note that in order to achieve the same radiation levels it is necessary to puff much more nitrogen than neon. That leads to strong core plasma contamination which is reflected in the much higher values of Z_{eff} and impurity concentrations in case of nitrogen. Nitrogen radiates mostly in the edge (SOL) region in contrast to neon where a large part of the plasma power is radiated within closed magnetic surfaces. With nitrogen the plate temperature is higher which could lead to strong local heat loads as well as erosion rates. However, the total eroded carbon flux is almost the same for both species.

The present ITER-like JET magnetic configuration is characterized by a strong asymmetry in the divertor regarding the x-point-to-target distance: the inner divertor target plates are relatively close to the x-point position in contrast to the outer divertor where the x-point target distance is large. In order to assess the effect of the divertor depth (≡ x-point to target distance along field line) a series of simulations has been done in which the distance along magnetic field line between divertor entrance (x-point) and divertor target plate has been changed.

In Fig. 5 we show some plasma parameters as a function of divertor depth. We note that the results presented in Figs. 3 and 4 have been achieved assuming 10 m distance between x-point and divertor target. Taking into account our simplified SOL geometry (slab model) the results presented here should be treated qualitatively only.

It emerges from the simulation results that the discharge parameters can be strongly affected by the divertor depth. If the divertor is relatively deep and impurity neutrals are kept close to the target, then the plasma parameters in the core as radiation, Z_{eff} and impurity concentration weakly depend on the x-point to divertor distance. But if the distance is below some threshold, then the core plasma is strongly affected by impurities. Z_{eff} increases strongly as well as plasma radiation since impurity neutrals are able to penetrate directly to the core plasma.

3. Conclusions and future plans

The numerical code COREDIV aimed at a self-consistent description of core and edge regions in tokamaks has been developed. The code is able to reproduce some aspects of the neon-seeded AT JET discharges of the 2007 experimental campaigns, in particular the core properties. COREDIV assumes a symmetric divertor and reproduced heat loads to the outer target plates. However, the predictions as they are for a 'divertor depth' of 10 m do not predict what is seen at the inner divertor. Namely there was essentially no decrease in power to inner divertor tiles with increasing f_{rad}. To approximate the inner divertor within the code would be necessary to go to an asymmetric SOL model. In fact, one sees from Fig. 5 that for divertor depths less than 8 m the radiated power rises dramatically for the given neon flux due to core pollution as seen in the Z_{eff} plot. That indicates a possible strong influence of the inner divertor region on the overall energy balance. Therefore, in order to correctly account for the heat load distribution to both divertors, simultaneous treatment of inner and outer SOL is indispensable. That would be the direction of future code developments.

Simulations with nitrogen indicate that neon is preferred to nitrogen within the considered range of the parameters since it leads to lower contamination and smaller heat loads to the target.

Acknowledgements

This work, supported by the European Communities under the contract of Association between EURATOM and IPPLM, was carried out within the framework of the European Fusion Development Agreement. The views and opinions expressed herein do not necessarily reflect those of the European Commission.

References

[1] R. Stankiewicz, R. Zagórski, J. Nucl. Mater. 337–339 (2005) 191.
[2] R. Zagórski et al., Contrib. Plasma Phys. 48 (1–3) (2008) 179.
[3] J. Rapp et al., J. Nucl. Mater. 337–339 (2005) 826.
[4] J. Mandrekas, W.M. Stacey, Nucl. Fusion 35 (1995) 843.
[5] Y. Shimomura et al., Fusion energy, in: Proceedings of the 18th International Conference, Sorrento, IAEA, Vienna, 2000. (CD-ROM ITER/1 and <http://www.iaea.org/programmes/ripc/physics/fec2000/html/node1.htm>).
[6] S.I. Braginskii, Rev. Plasma Phys. 1 (1965) 205.
[7] M. Leigheb et al., J. Nucl. Mater. 241–243 (1997) 914.
[8] J. Roth et al., J. Nucl. Mater. 337–339 (2005) 970.